

	Simulation of the elastic wave propagation induced by the PS beam into the TOF target at CERN	TOF MSS Prj FINAL REPORT	Page 1/27
---	---	--------------------------------	-----------

# Simulation of the elastic wave propagation induced by the PS beam into the TOF target at CERN

G. Fotia, F. Maggio, L. Massidda

*CRS4, Centre for Advanced Studies, Research and Development in Sardinia*

S. Buono

*CRS4 and CERN, European Organization for Nuclear Research*

## 1 Introduction

The TOF lead target, currently under commissioning at CERN, undergoes relevant temperature and stress transients due to the intensity of the incident beam ( $20 \text{ GeV}/c$ ). A pulse of  $7 \times 10^{12}$  protons carries in fact an energy of  $21.4 \text{ kJoule}$  delivered in  $7 \text{ ns}$ . In the actual beam size and distribution, this causes a maximum theoretical (adiabatic) temperature increase of  $34.4 \text{ K}$  inducing a relevant dynamic transient [1].

The load history of the target is periodic, with up to four pulses heating the target for each super-cycle of  $14.4 \text{ s}$ , with a minimum pulse separation of  $1.2 \text{ s}$  to allow heat transfer. In these conditions the average beam current would be equal to  $0.31 \text{ mA}$ , with an energy deposit per super-cycle of  $85.6 \text{ kJoule}$  and an average beam power of  $3.0 \text{ kW}$  (only the 51% of the beam is deposited on the target).

Therefore, if it is important to evaluate the operating temperatures induced in the target in a quasi stationary or transient situation, on the other hand the dynamic transient due to the propagation of elastic waves and the corresponding stresses induced appears to be of importance in order to assess the occurrence of a mechanical failure.

## 2 General assumptions

The structure of the target has an overall dimension of  $80 \times 80 \times 60 \text{ cm}$  with a brick shape except for the central spallation area, where a volume of  $30 \times 55 \times 20 \text{ cm}$  is removed to have the nominal design dimension.

	Simulation of the elastic wave propagation induced by the PS beam into the TOF target at CERN	TOF MSS Prj FINAL REPORT	Page 2/27
---	---	-----------------------------	-----------

The structure, made of pure lead, is not monolithic but composed by a set of 9 independent blocks, not joined in any way, but closely packed together. This assembly is completely submerged by water with a minimum thickness of 5 cm all around the surface of the block, and everything is contained by an aluminum alloy vessel.

The energy deposition of the beam is focused on the central block of the lead target. In this block the temperature raise causes a state of internal stress that propagates in the target as an elastic wave: this is by far the part subjected to the most significant load. For this reason, the analysis of the elastic wave propagation is first confined to this central block, also to avoid to give rise to exceedingly large computational problems. The boundary conditions on the block should take into account the effective gap between blocks, and on the behavior of the liquid in between. Two opposite conditions of free surface and absorbing boundaries are considered and implemented.

Very different time scales are involved for energy deposition ( $10^{-8}$  s) wave propagation ( $10^{-3}$  s) and heat transmission ( $10^0$  s), thus suggesting two simplifying assumptions on the load mechanism.

Since the simulation time is by far low in respect to the minimum spacing between subsequent incident pulses, and also for appreciable variations of the material temperature due to heat transmission, we limit to examine the effect of a single pulse. Furthermore the temperature distribution and the thermal expansions in the material will be considered constant during all the simulation time.

On the other hand, the temperature rise is distributed in a time of a few ns, much lower than the wave propagation characteristic times for the given geometry: therefore it makes sense to consider the load as a step rising, and the energy deposition as a perfect impulse.

In order to make the temperature rise independent from the chosen time step, the rise is applied as an initial condition: the simulation starts from a non equilibrium condition in which the thermal load and consequently the pressure load and the deposited energy, are absorbed neither in the form of potential energy of the elastic deformation nor in the form of kinetic energy of the material movement.

### 3 Spectral elements analysis

The analysis was performed on a modified version of the spectral element code ELSE, developed at CRS4 [2].

ELSE (ELasticity by Spectral Elements) is a numerical solver for linear elastodynamics in the approximation of small displacements, based on spectral elements of Legendre type; stems from a Galerkin method coupled with a non-overlapping domain decomposition in quadrilaterals (2-D) or hexahedra (3-D)

The spectral elements method can provide greater accuracy with a lower number of grid points per wave length compared with a standard finite element method, allowing faster analysis. In some situation it gives the possibility to treat problems that are beyond the limits of finite elements with the current computing systems.

#### 3.1 Properties of the material

The central block of the target is entirely made of pure lead. For modeling purposes it has been considered as an isotropic linear elastic material, whose physical properties do not depend from temperature and kinetic effects. The values used in the calculations are listed in the following table.

Table 1 Lead mechanical and thermal properties

Density	$\rho$	11340	kg/m <sup>3</sup>
Young modulus	E	14000	MPa
Poisson ratio	$\nu$	0.3	-
Damping viscosity	$\gamma$	0.0	Pa s
Thermal expansion coefficient	$\alpha$	29.1 10 <sup>-6</sup>	K <sup>-1</sup>
Specific heat	Cv	129.0	J/kg/K

### 3.2 Geometry

The geometry of the block under analysis is extremely simple, being composed of a brick, whose dimension and orientation are shown in Figure 1.

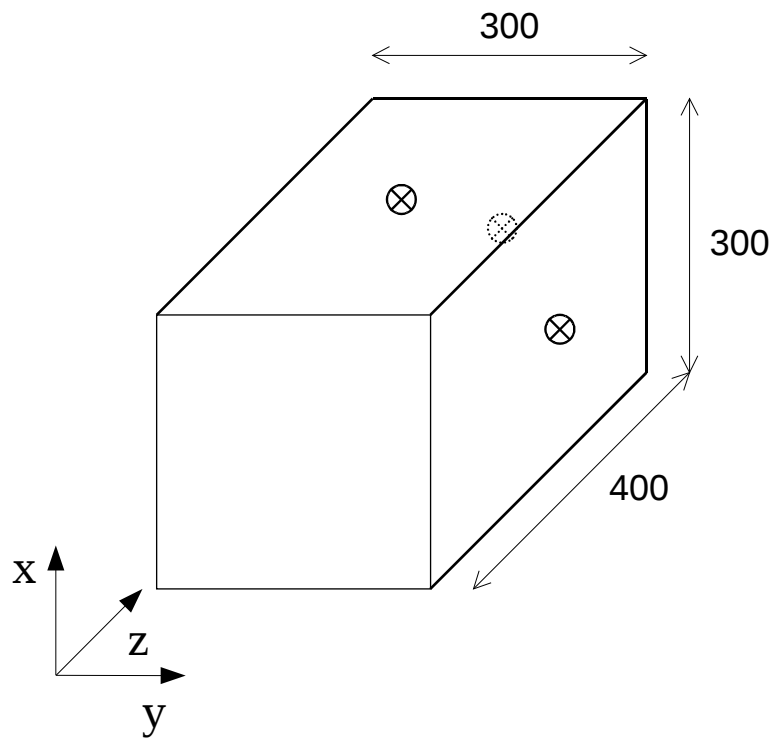


Figure 1 Geometry of the block (lengths expressed in mm)

The coordinate frame is oriented as shown in the figure and its origin is placed in the lower left corner of the front face of the block.

### 3.3 Spectral element model

The spectral element model is composed by a regular mesh of hexahedral elements. The block is decomposed in 40x40x40 elements (64000 total), each with the following dimensions: 7.5 mm along the x and y axes and 10 mm along the z axis. The minimum internodal distance is around 2 mm.

	Simulation of the elastic wave propagation induced by the PS beam into the TOF target at CERN	TOF MSS Prj FINAL REPORT	Page 4/27
---	---	-----------------------------	-----------

The elements are discretized by means of polynomial functions of degree 3 (in each direction), corresponding to *4 nodes* on each edge, *16 nodes* on each face and *64 total nodes* for each element. The implementation is based on a structured approach, in which nodes corresponding to common faces are replicated: therefore the total number of nodes is equal to *4096000* and more than *12 million* unknowns resulted.

The grid size appears to be adequate to describe the energy deposition of the heating pulse and to describe wave lengths corresponding to frequencies up to *100000 Hz*.

In Figure 2 a scheme of the meshing adopted and of the nodal position for a generic element are shown.

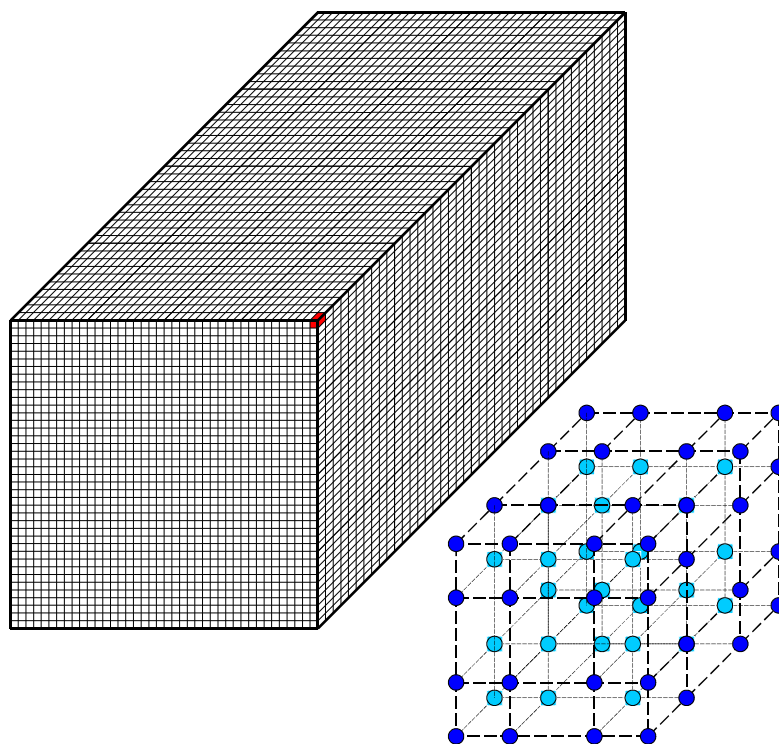


Figure 2 The computational grid: element distribution (left) and nodes inside a generic element (right)

### 3.4 Boundary conditions

Two different kind of boundary conditions are set to the central block. First the external faces of the block are in fact considered free to vibrate, neglecting the existence of other material surrounding the block and confining the elastic energy inside the block. In a second step absorbing boundary conditions, in the Stacey formulation, are set: they simulate continuity with a surrounding material of the same nature of the block studied, and cause the elastic energy to be approximately absorbed by the boundaries of the computational domain as if it would be transferred to the surrounding medium.

The real conditions (contact and presence of water) are hard to formulate and harder even to simulate: the lateral surfaces, normal to the *y* axis may not be in direct contact with other blocks since a gap of unknown measure filled with water could exist; the front and back surfaces are in direct contact with water and wave transmissibility between the two media should be simulated;

	Simulation of the elastic wave propagation induced by the PS beam into the TOF target at CERN	TOF MSS Prj FINAL REPORT	Page 5/27
---	---	-----------------------------	-----------

finally, upper and lower faces, perpendicular to the x axis, are in direct contact with other lead blocks: because of their weight one may think that the continuity is assured and therefore the absorbing boundary conditions are closer to the real physical condition, but more realistically one should introduce an unilateral contact bringing a serious non-linearity in the simulation.

The real conditions reasonably stay somewhere between the two extremes, we think probably nearer to absorbing boundaries than to free boundaries condition, so that a significant part of the elastic energy is propagated outside the central block.

### 3.5 Heat generation loads

During beam impact the lead target is subjected to internal heat generation, characterized by an extremely short time of energy deposition. As mentioned before, we make the assumption that energy deposition is instantaneous when compared to the characteristic times of wave propagation; the temperature rise and thermal expansion are considered instantaneous as well.

The energy deposition is applied to the spectral elements model starting from the data of a FLUKA simulation, where the energy deposition of the beam per single  $20 \text{ GeV}/c$  proton is given.

The FLUKA mesh we used for the simulation is coarse when compared with the spectral mesh; thus in order to avoid a stepped energy distribution, an interpolation procedure has been carried out: an auxiliary mesh of eight nodes bricks, with nodes placed in the centers of the FLUKA cells was created, and the energy deposition for each node of the spectral mesh was calculated using standard finite element shape functions. The result is a smoother energy profile with limited consequences on the value of maximum energy peak.

From the distribution of the local energy deposition on the spectral nodes, the local temperature rise is calculated by dividing the energy density  $E_d$  for the specific heat  $C_v$  and the material density  $\rho$ :

$$\Delta t(x, y, z) = \frac{E_d(x, y, z)}{\rho C_v}$$

This will give rise to an immediate thermal expansion of the material depending from the local temperature rise  $\Delta t$  and the thermal expansion coefficient  $\alpha$ :

$$\varepsilon_{xx}^{th} = \varepsilon_{yy}^{th} = \varepsilon_{zz}^{th} = \alpha \Delta t$$

This state of deformation is not in equilibrium and causes an internal stress state; the consequent elastic deformation  $\varepsilon^e$  is equal and opposite to the thermal deformation, resulting in a vanishing total deformation. The material is supposed to have a linear elastic behavior according to the following law, in which  $C$  is the stress strain matrix,  $\varepsilon$  is the effective total deformation sum of the elastic and thermal part, and  $\sigma$  is the resulting stress:

$$\sigma = C(\varepsilon - \varepsilon^{th}) \quad \sigma = C(\varepsilon - \varepsilon^{th})$$

The thermal expansion originates therefore a compression in the material and a pressure wave that propagates in the material starting from the energy deposition area.

### 3.6 Time steps, solution options and post-processing

As already mentioned, the significant duration of the simulation of the wave phenomenon is much shorter than the time required for a significant variation of the temperature profile due to heat

	Simulation of the elastic wave propagation induced by the PS beam into the TOF target at CERN	TOF MSS Prj FINAL REPORT	Page 6/27
---	---	-----------------------------	-----------

conduction, and very much shorter than the time span between subsequent pulses. Therefore a single pulse has been studied, and no thermal conduction has been considered.

The duration of the simulation has been chosen on the basis of the wave propagation velocity inside the lead and considering the block dimensions; the wave propagation velocity inside the material for normal and transverse waves are calculated starting from the Lamè coefficients,

$$\lambda = \frac{E\nu}{(1+\nu)(1-2\nu)} \quad \mu = \frac{E}{2(1+\nu)}$$

in the following way:

$$c_p = \sqrt{\frac{\lambda+2\mu}{\rho}} \quad c_s = \sqrt{\frac{\mu}{\rho}}$$

The results are summarized in the following table:

Table 2 Elastic properties and wave speed in lead material

Lamè coefficient	$\lambda$	8077	MPa
Lamè coefficient	$\mu$	5385	MPa
Density	$\rho$	11340	kg/m <sup>3</sup>
Perpendicular wave speed	$c_p$	1289	m/s
Transverse wave speed	$c_s$	689	m/s

Since the maximum sound speed in lead is about  $1300 \text{ m/s}$  and the minimum travel for an elastic wave propagating from the center is  $0.150 \text{ m}$  to reach the border of the block, the time is around  $1.2 \cdot 10^{-4} \text{ s}$ , a simulation time of  $1.0 \cdot 10^{-3} \text{ s}$  will be adequate both for absorbing boundary conditions, since the elastic waves would completely exit outside the block, and also for free boundary conditions, since it will be possible to capture several wave reflections.

Since the code uses an explicit central difference scheme for time advancing, the time step is limited by the stability condition, that puts an upper limit around  $1.4 \cdot 10^{-6} \text{ s}$ . For safety and accuracy reasons a time step of  $0.5 \cdot 10^{-6} \text{ s}$  has been chosen.

Dedicated preprocessors and postprocessors are available: the latter provide nodal displacements and nodal stresses at chosen time step. The time history of the displacements of the central points of the six faces of the block can be extracted. Several snapshots of the nodal displacements, of the components of the nodal stresses, and of the equivalent stresses in terms of pressure and Von Mises equivalent stress have been saved, moreover the temperature distribution is saved for check. These results have been elaborated via specific postprocessors to obtain plots of different cross sections.

## 4 Results

As mentioned before the energy deposit input is taken from a FLUKA simulation result. This energy is distributed over the block volume and the instantaneous temperature increase is calculated; the plots in Figure 3 show the temperature increase distribution in two sections of the central block, one normal to the  $z$  direction and passing through the point of maximum energy deposition and the other normal to the  $x$  direction, and passing through the center of the block and

the point of maximum energy deposition too. The results appear to be in good accordance with those of other heat conduction simulations [3].

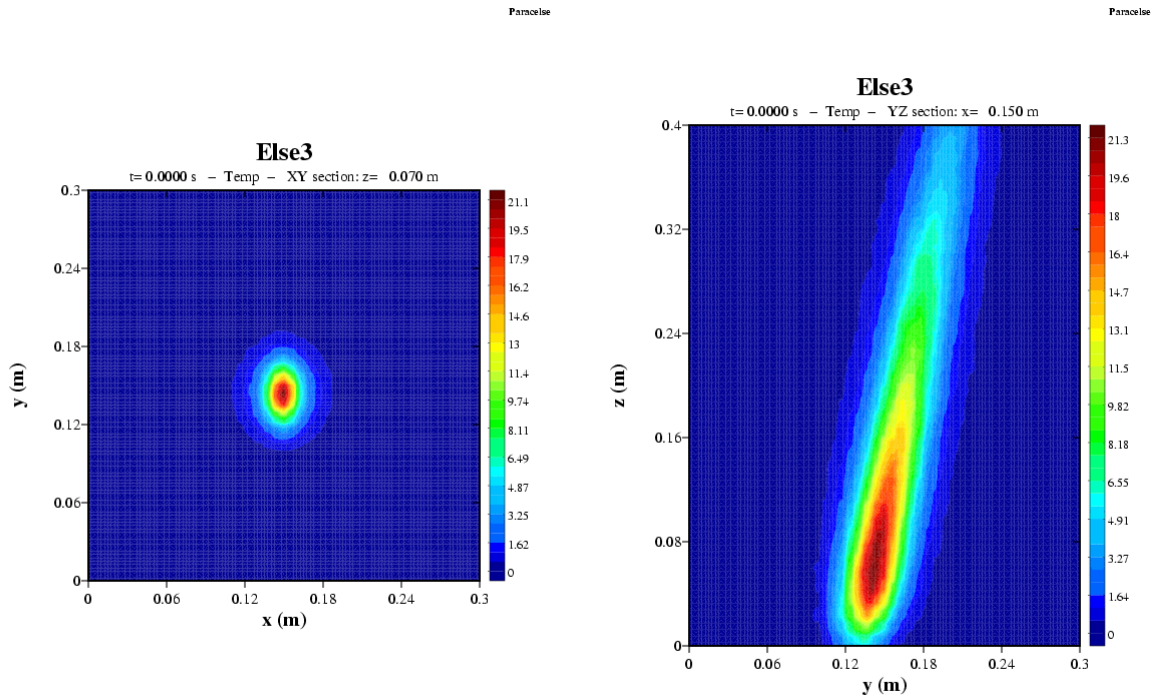


Figure 3 Initial temperature distribution in the central block

This temperature distribution is the loading condition for both the following simulation: with absorbing and free boundaries.

#### 4.1 Absorbing boundary conditions

The plot in Figure 4 shows the normal component of the displacement of three points located at the center of the external faces of the central block as shown in Figure 1: the displacement along the  $x$  direction for the face parallel to the  $yz$  plane (the top face), the  $y$  component of the displacement for the face parallel to the  $xz$  plane (the right face), and the  $z$  component for the  $xy$  face (the back face).

Due to the energy and temperature distribution, the wave effect is more evident for the lateral and top surface of the block than for the back one, and the absorbing boundary condition do not allow reflection of the waves on the block surfaces, therefore only one peak is evident.

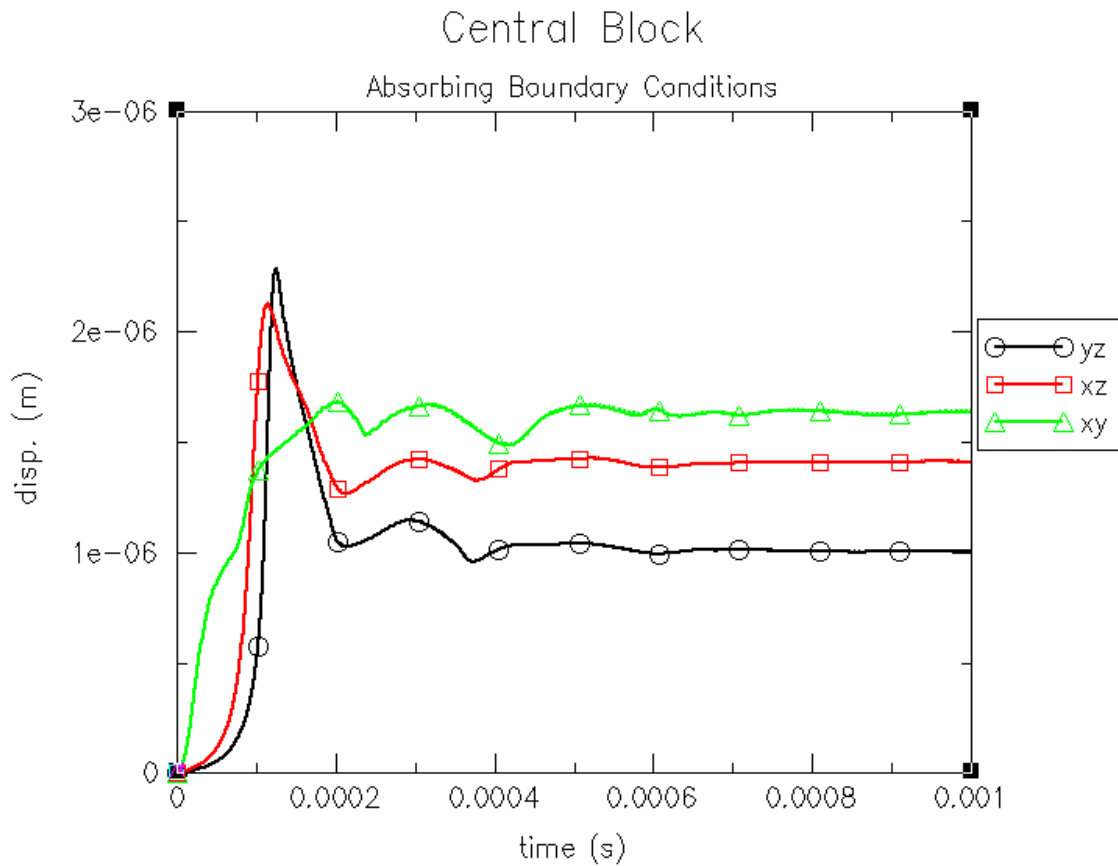


Figure 4 Normal displacement of the central point of the block faces

This is also evident in the snapshots from Figure 5 to Figure 8 where the pressure distribution in two sections of the central block (the same of the temperature plots) is shown at several times. The pressure wave crosses the boundaries of the block with no reflection.

It can be clearly appreciated that the maximum values of the pressure in the material occur at the same point of the maximum energy deposition, and the pressure wave propagating has a much lower intensity. Pressure has the highest value at the pulse deposition time, when reaches values up to 210 bar.

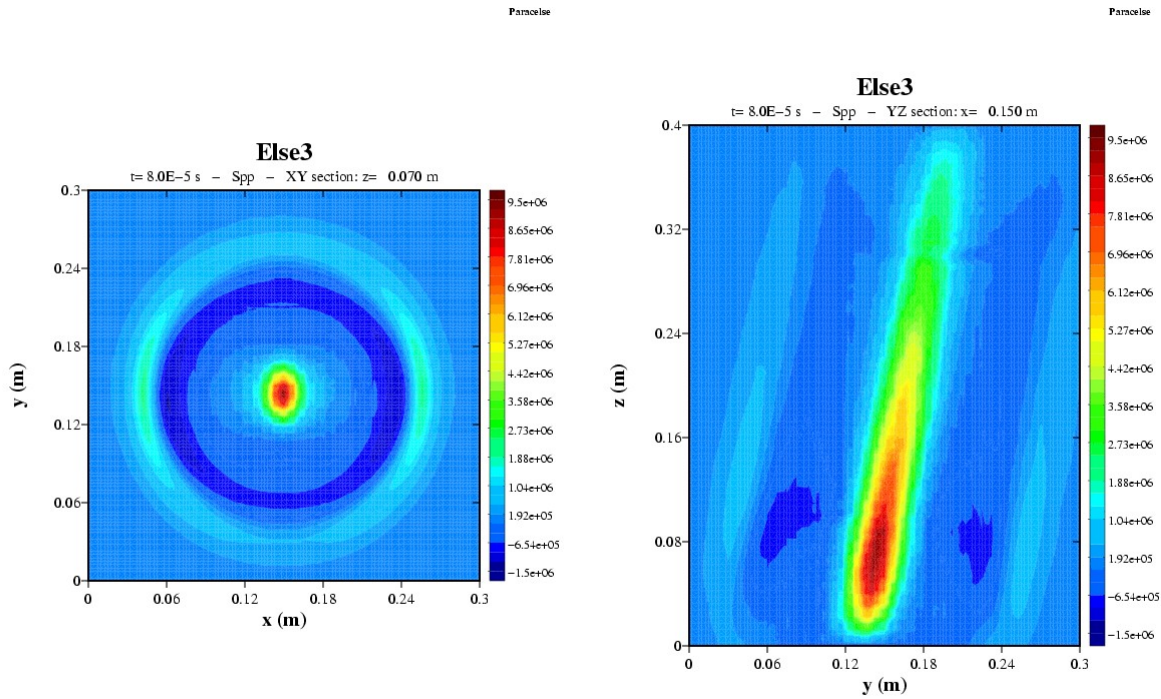


Figure 5 Pressure in two sections of the central block (Pa)

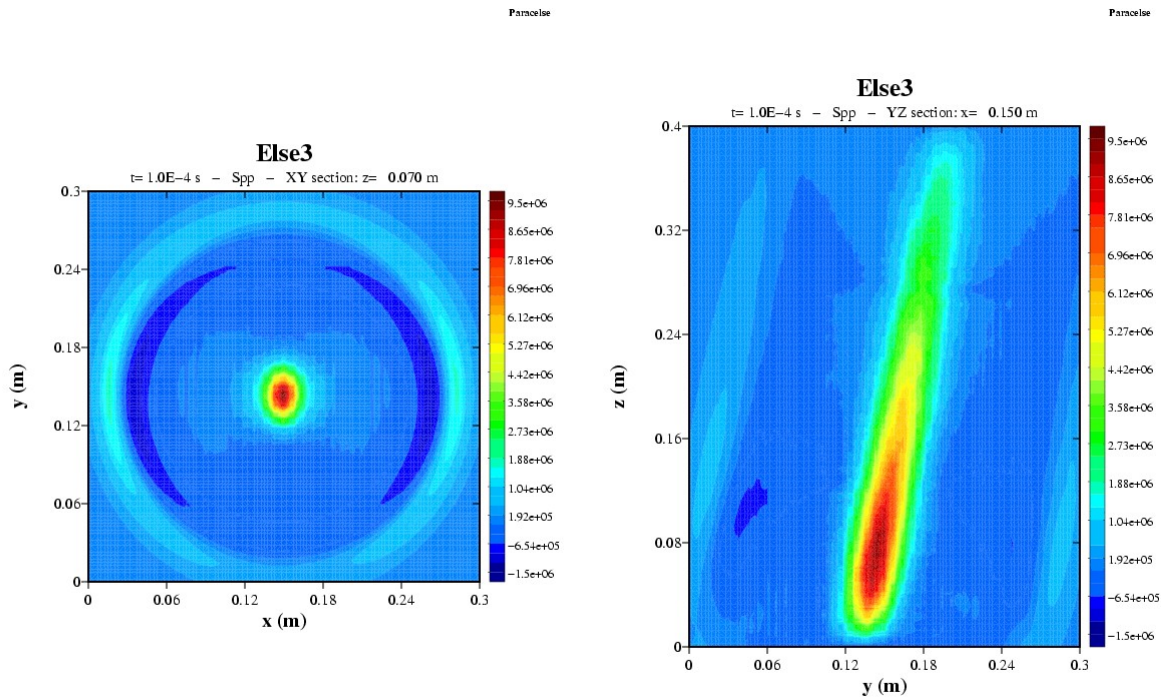


Figure 6 Pressure in two sections of the central block (Pa)

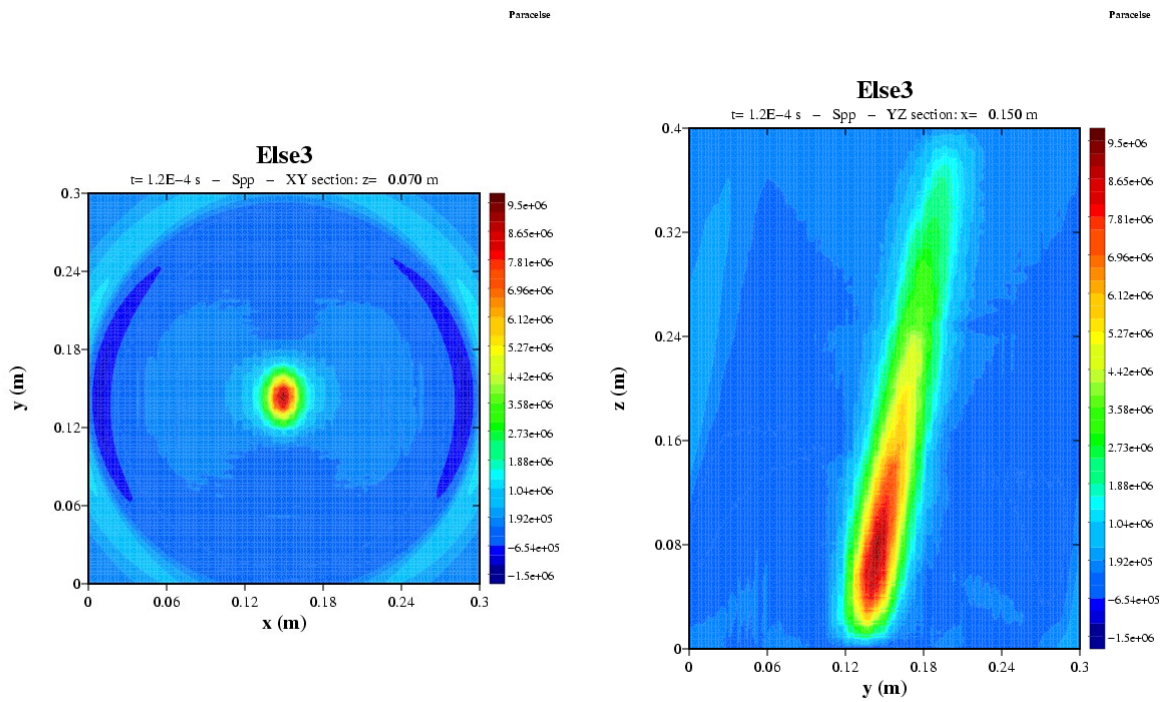


Figure 7 Pressure in two sections of the central block (Pa)

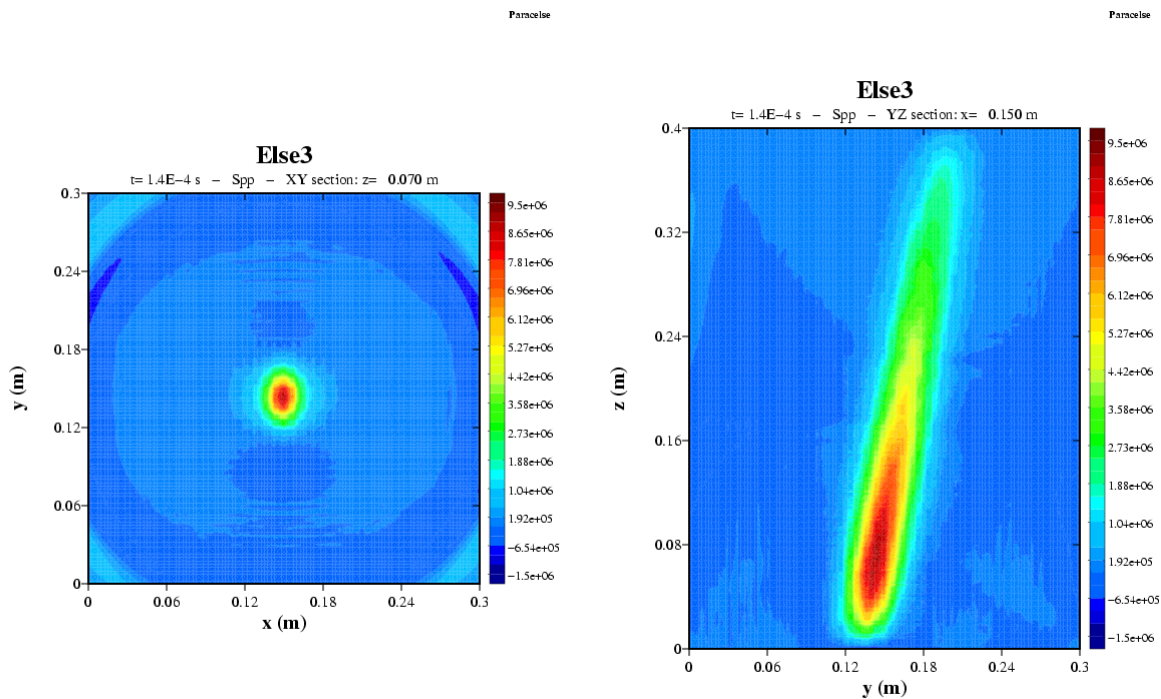


Figure 8 Pressure in two sections of the central block (Pa)

The Von Mises equivalent stress, taken as parameter to assess the material stability, has much lower values. The plots in Figure 9 and Figure 10 show its values at different times for the  $xy$  section of the block. The peak values is still at the maximum energy deposition point and equals  $8.3 \text{ MPa}$  at the instants immediately following the pulse impingement.

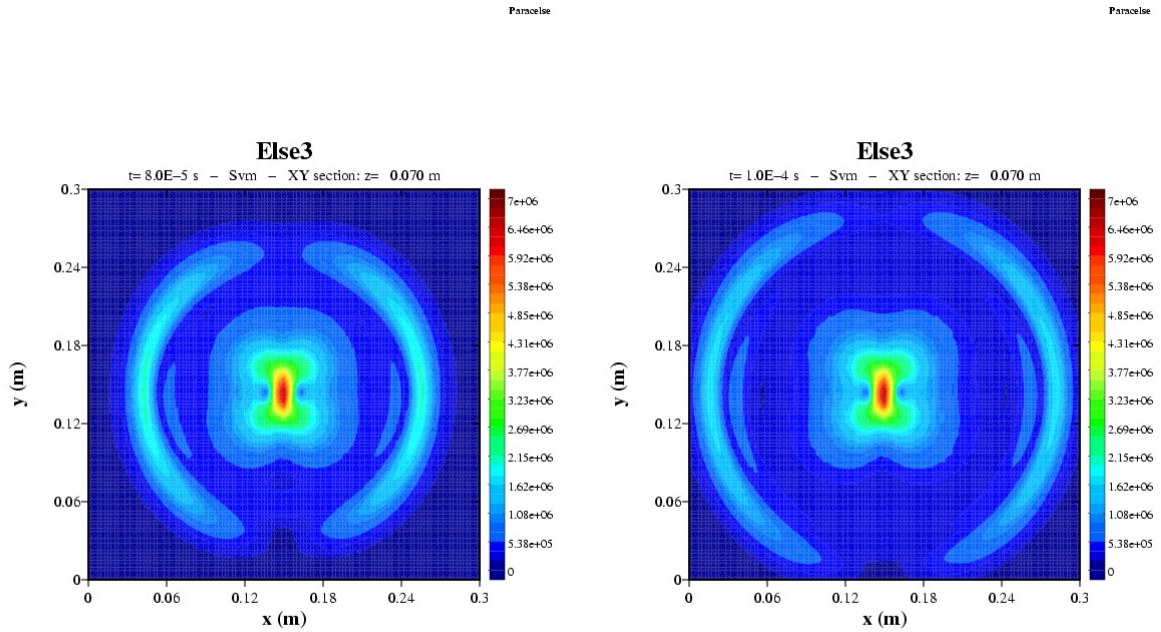


Figure 9 Von Mises equivalent stress in a section of the central block (Pa)

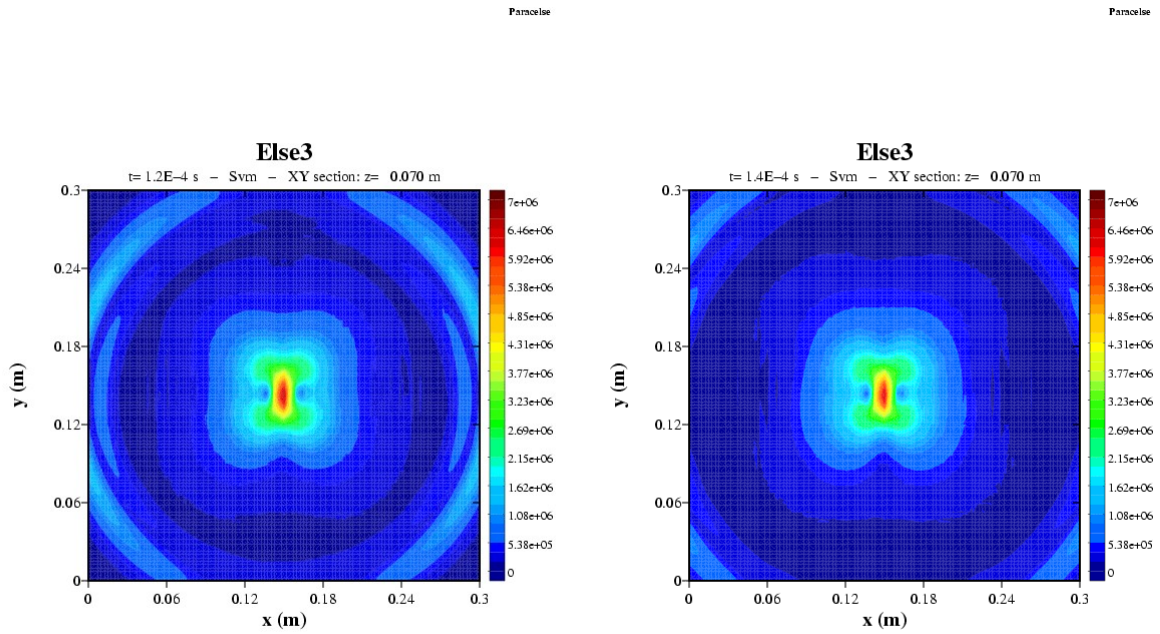


Figure 10 Von Mises equivalent stress in a section of the central block (Pa)

## 4.2 Free boundary conditions

The diagram in Figure 11 shows the normal displacements of the central points of the block faces when free boundary conditions are set. In this case, the effect of multiple reflections inside the block is evident: the energy associated with the wave propagation is confined inside the block and the maximum displacement appears to be higher than the previous analysis.

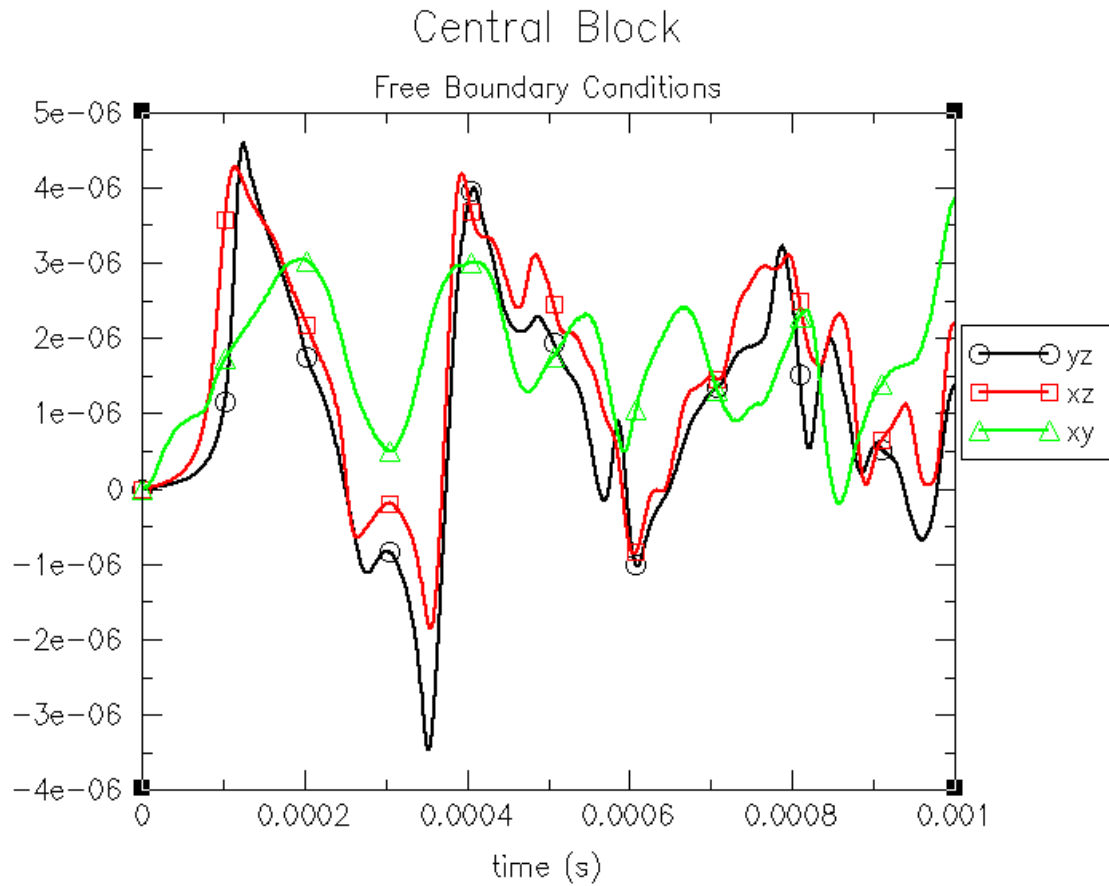


Figure 11 Normal displacement of the central point of the block faces

Plots in Figure 12 to Figure 15 show the pressure in two sections of the block. The pressure values associated with the wave are higher than those found when setting absorbing boundary conditions, but they are still lower than the peak value at maximum energy deposition point. As the wave travels away from the source point it spreads its energy in a larger volume, rapidly decreasing its intensity: the reflection of the already weak wave cannot give rise to much high pressure peaks.

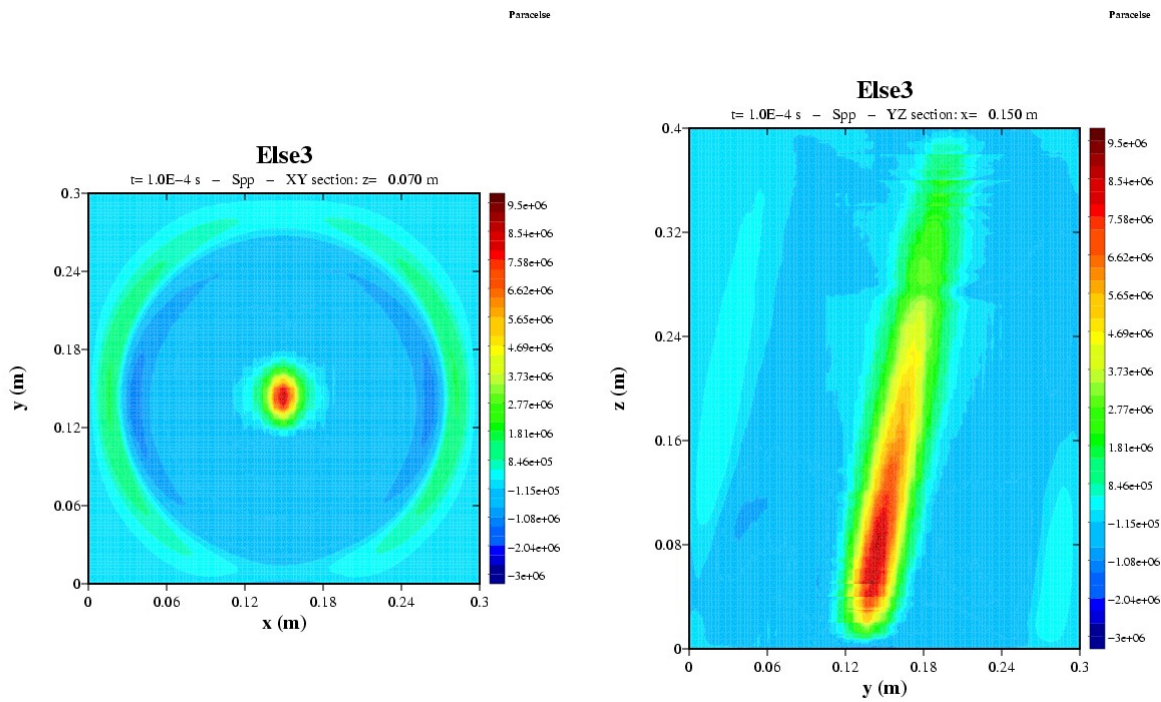


Figure 12 Pressure in two sections of the central block (Pa)

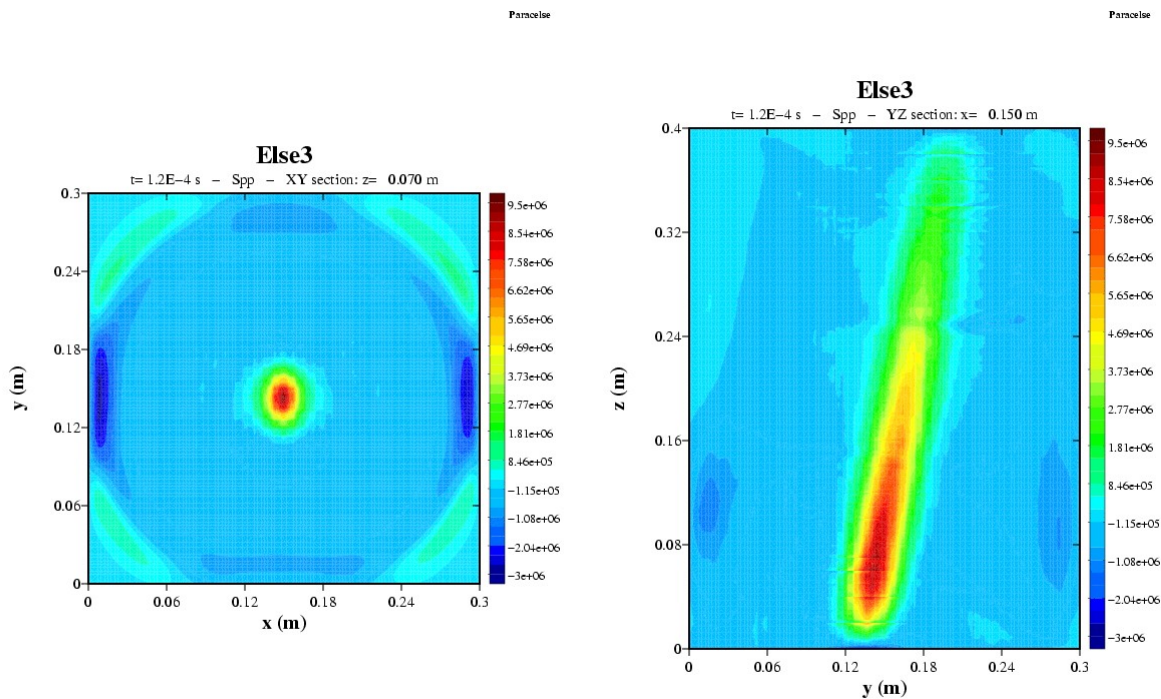


Figure 13 Pressure in two sections of the central block (Pa)

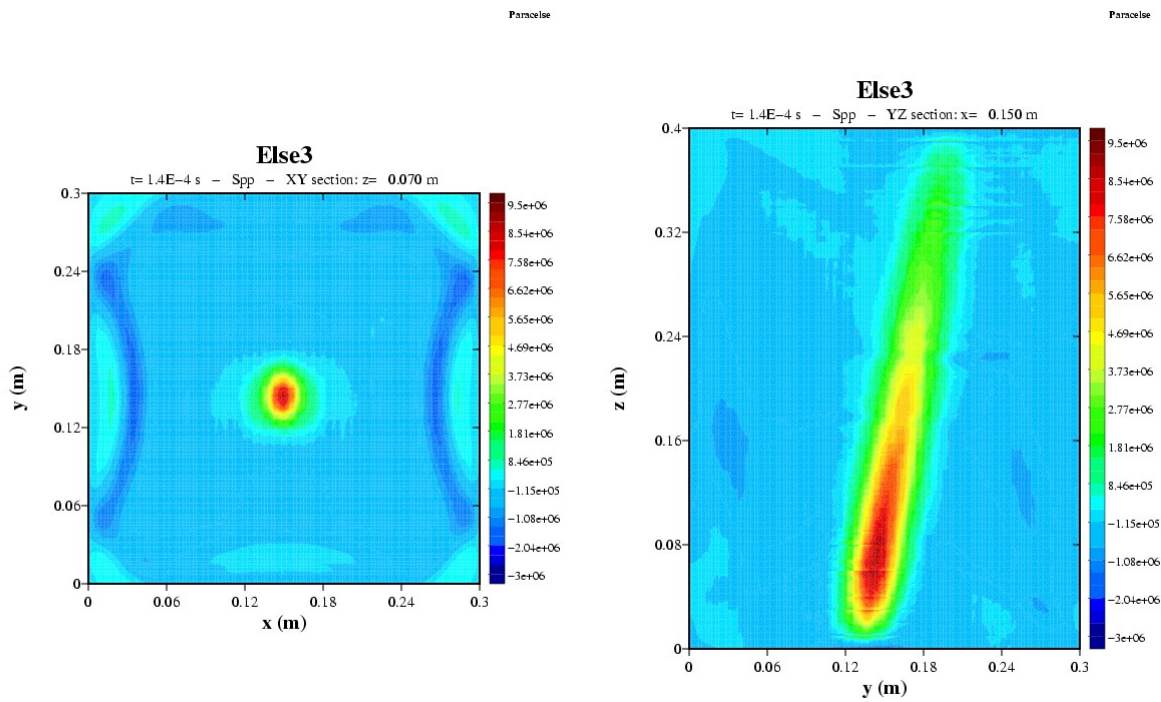


Figure 14 Pressure in two sections of the central block (Pa)

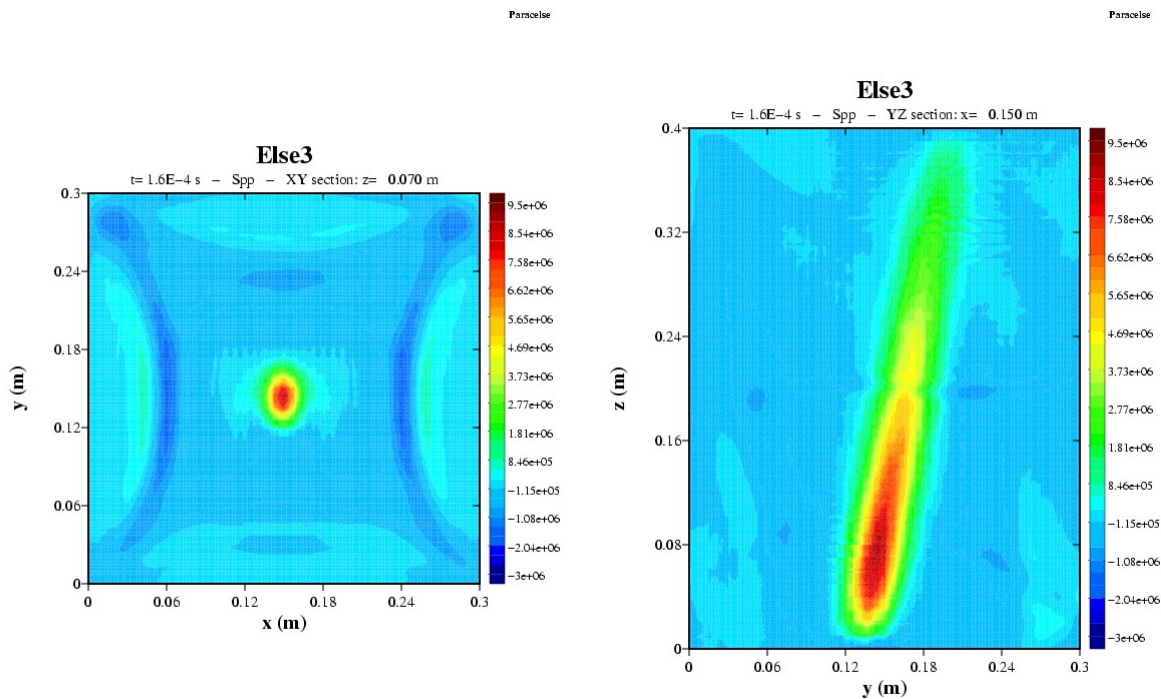


Figure 15 Pressure in two sections of the central block (Pa)

Finally, in the plots of Figure 16 and Figure 17 the Von Mises equivalent stress in the points of the xy section is plotted: its values, although higher than for the absorbing boundary case, are still much lower than pressure values, with the peak concentrated in the maximum temperature point.

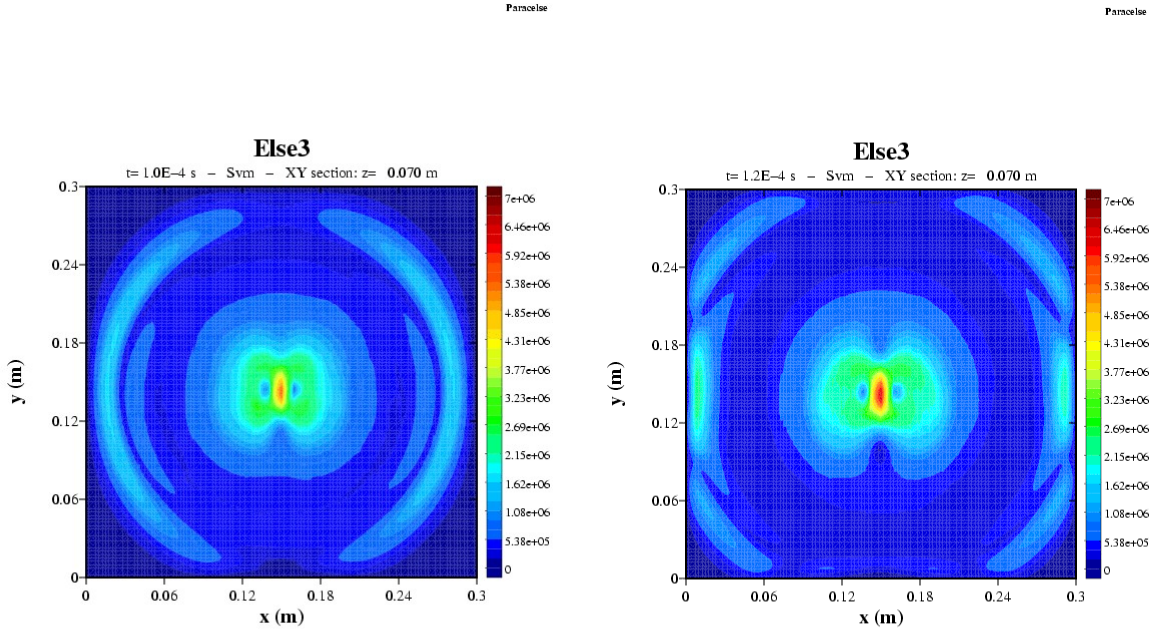


Figure 16 Von Mises equivalent stress in a section of the central block (Pa)

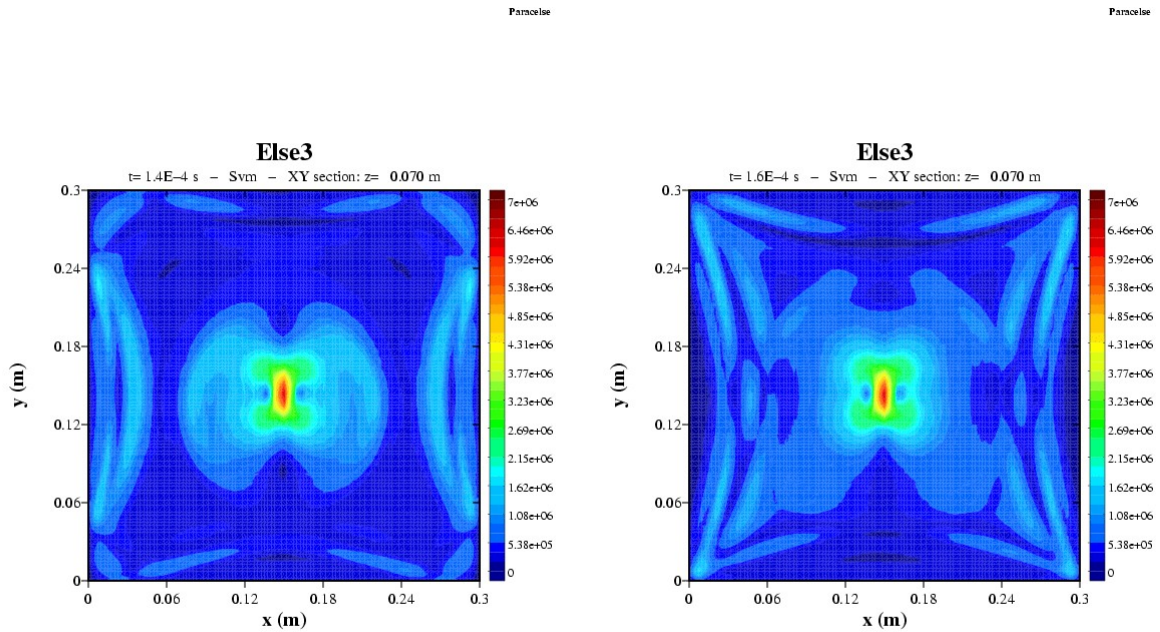


Figure 17 Von Mises equivalent stress in a section of the central block (Pa)

## 5 2D section

As a further analysis we investigated the behavior of a section of the entire target, including, with several approximations, the water surrounding the lead target and the aluminum container.

Continuity between the lead blocks is assumed, and the effect of gaps between the blocks and of the unilateral contact has not been considered.

We used the same heat input source, “adapted” by interpolation on the spectral element mesh; the section to be analyzed was chosen to intersect the energy deposition volume in peak section.

Figure 18 shows a sketch of the model adopted for the target section and its boundary conditions.

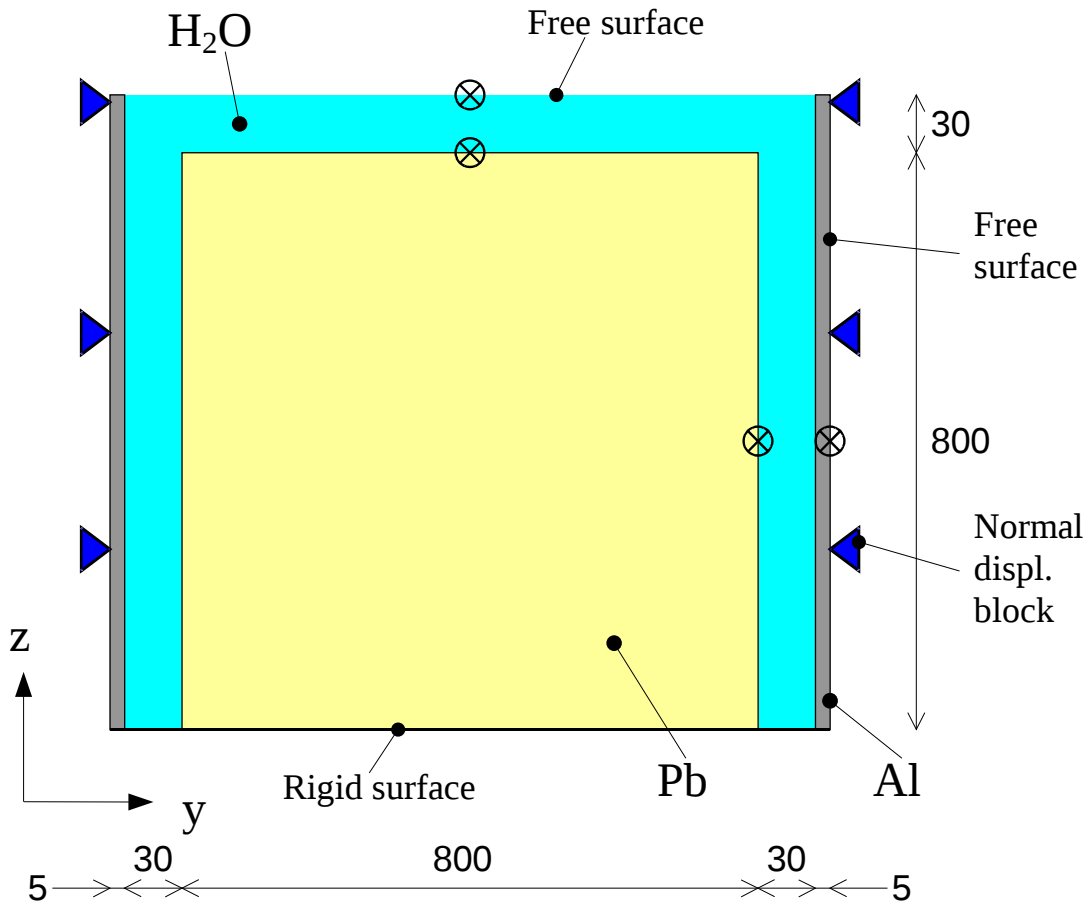


Figure 18 Geometry of the target section and boundary conditions (lengths expressed in mm)

The lead block has a square section with a side length of 800 mm, and it is surrounded everywhere except on the bottom side by a 30 mm thick layer of water, everything is contained in an aluminum box 5 mm thick.

The top surface of the liquid is considered free, as well as the right and left sides of the aluminum container. On this sides additional boundary conditions blocking normal displacement at the surface are added to simulate the presence of stiffening plates surrounding the container. Finally the bottom surface is assumed to be rigid.

Due to the nature of the problem, we assumed it could be reasonable to simulate the liquid as an elastic material, neither transport nor viscosity is included in the model, and this pseudo-elastic material does not have tangential stiffness, so that can only propagate normal waves.

The properties of the lead are the same previously described; the following table shows the assumed properties for aluminum.

Table 3 Mechanical and thermal properties of aluminum

Young modulus	E	68700	MPa
Poisson ratio	$\nu$	0.3	-
Lamè coefficient	$\lambda$	39634	MPa
Lamè coefficient	$\mu$	26500	MPa
Damping viscosity	$\gamma$	0.0	Pa s
Thermal expansion coefficient	$\alpha$	$24.0 \cdot 10^{-6}$	$K^{-1}$
Specific heat	$C_v$	900	J/kg/K

Densities and wave velocities for aluminum and water are summarized in the following table.

Table 4 Properties of aluminum for wave propagation

Density	$\rho$	2700	$kg/m^3$
Perpendicular wave speed	$c_p$	5857	m/s
Transverse wave speed	$c_s$	3132	m/s

Table 5 Properties of water for wave propagation

Density	$\rho$	1000	$kg/m^3$
Perpendicular wave speed	$c_p$	1441	m/s
Transverse wave speed	$c_s$	0.0	m/s

A 3D model has been used to run this analysis, the thickness of the model was limited to *20 mm*, using *2 elements* along the thickness. Suitable boundary conditions for face nodes, namely blocking of the displacements in *x* directions, have been adopted.

In the analysis plane the mesh is regular and composed by *174* along *y* and *166* along *z* square elements with a side of *5 mm*.

Each element has *4 nodes* per side in the *y* and *z* direction and *2 nodes* in the *x* direction (*32 nodes* per spectral element); the mesh was composed by *57768 elements* and *1848576 nodes*, giving rise to more than *5.5 millions degrees of freedom*.

The time step adopted is lower than that used in the previous simulations due to a lower internodal distance and higher wave speeds; the spectral element method we use is based on explicit time-marching scheme and therefore is subjected to the CFL constraint. As a result, a value of  $5.0 \cdot 10^{-7}$  s was adopted for a total simulation time of  $10^{-3}$  s, corresponding to 2000 time iterations.

## 6 Results

The plot of Figure 19 shows the normal displacements of the center of the top surface of the lead block and the liquid surface (these points are in Figure 18). As expected, first waves arriving on the free surface induce waves propagating along the liquid with their own frequency.

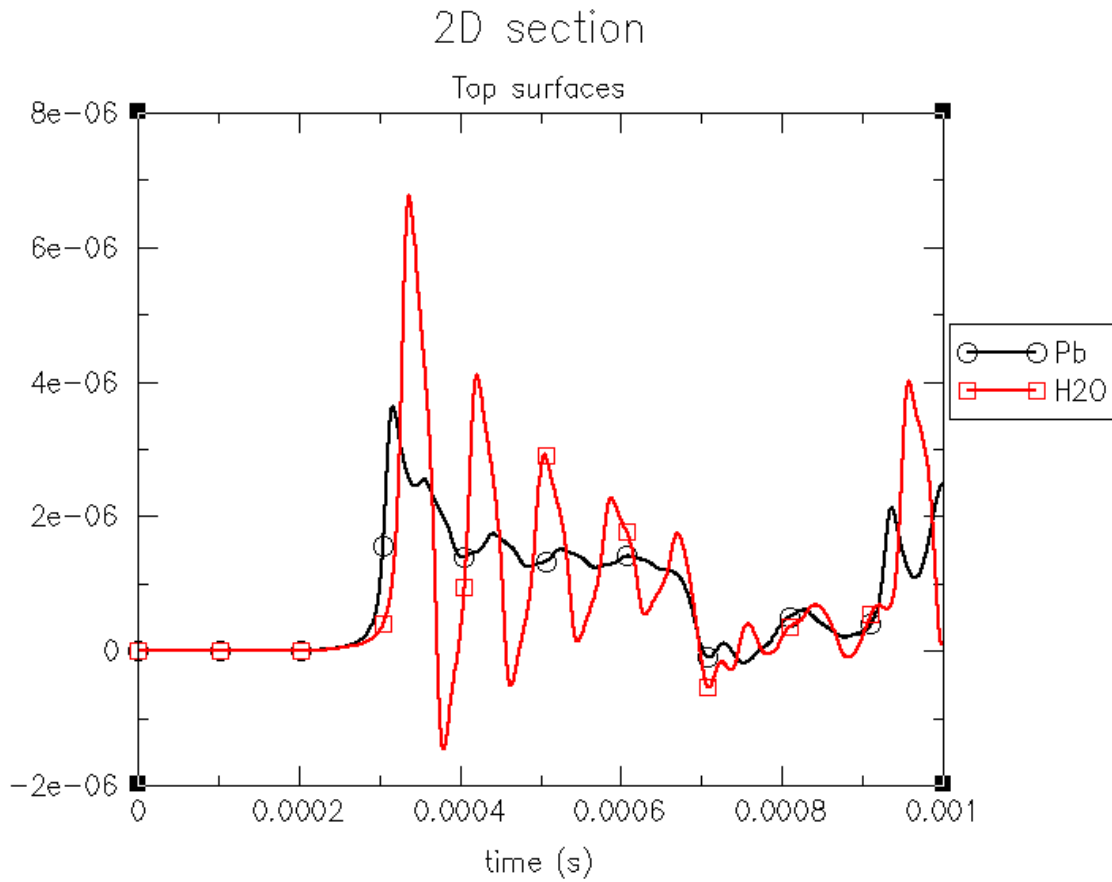


Figure 19 Displacements in Z direction for the central points of the top surfaces of the lead block and the water surface (m)

In Figure 20 displacements in y direction, i.e. normal to the aluminum surface, are plotted for the central point of the lead block and the external point of the aluminum container that faces it. The behavior is absolutely similar to that displayed in the previous plot.

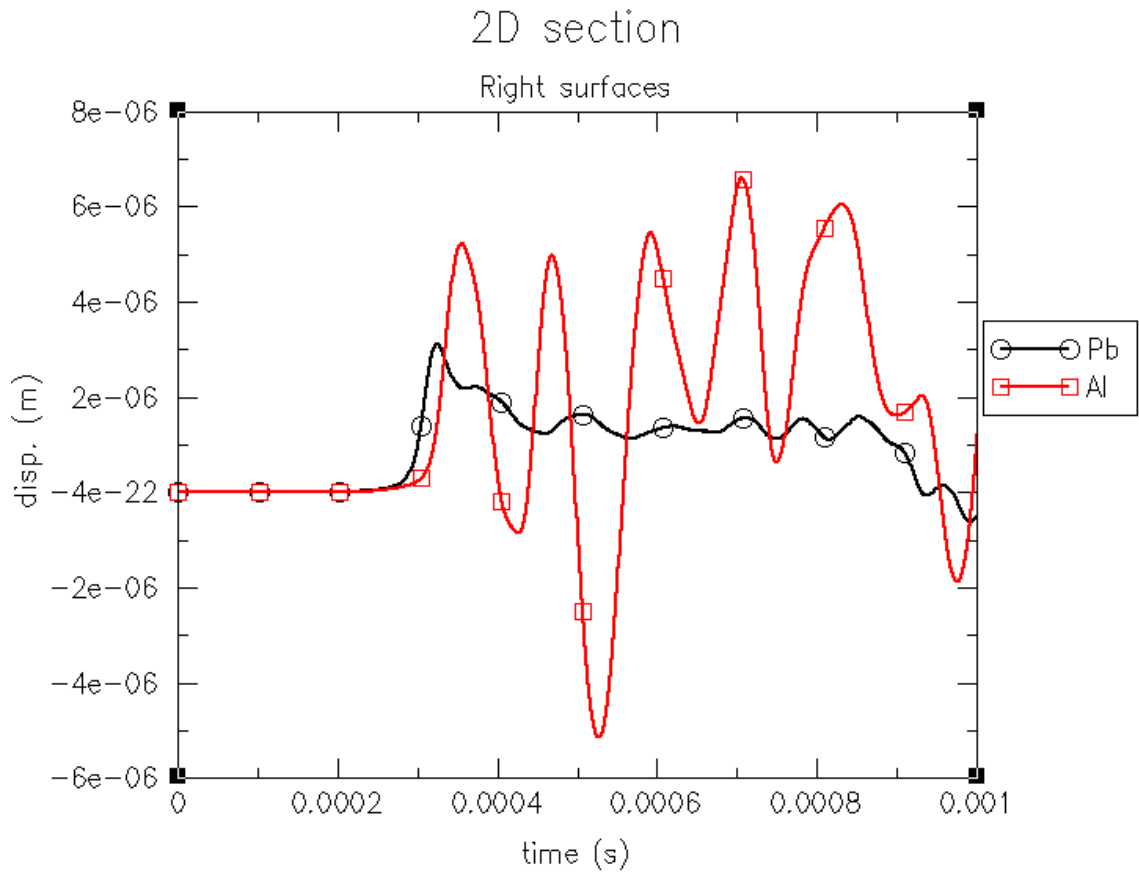


Figure 20 Displacements in Y direction for the central points of the right surfaces of the lead block and the Aluminum container (m)

Plots from Figure 21 to Figure 23 exhibit the pressure inside the target at different times. It is shown the arrival of the wave at the lead surface with partial reflections, and propagation in the surrounding materials and the subsequent evolution of the pressure wave distribution.

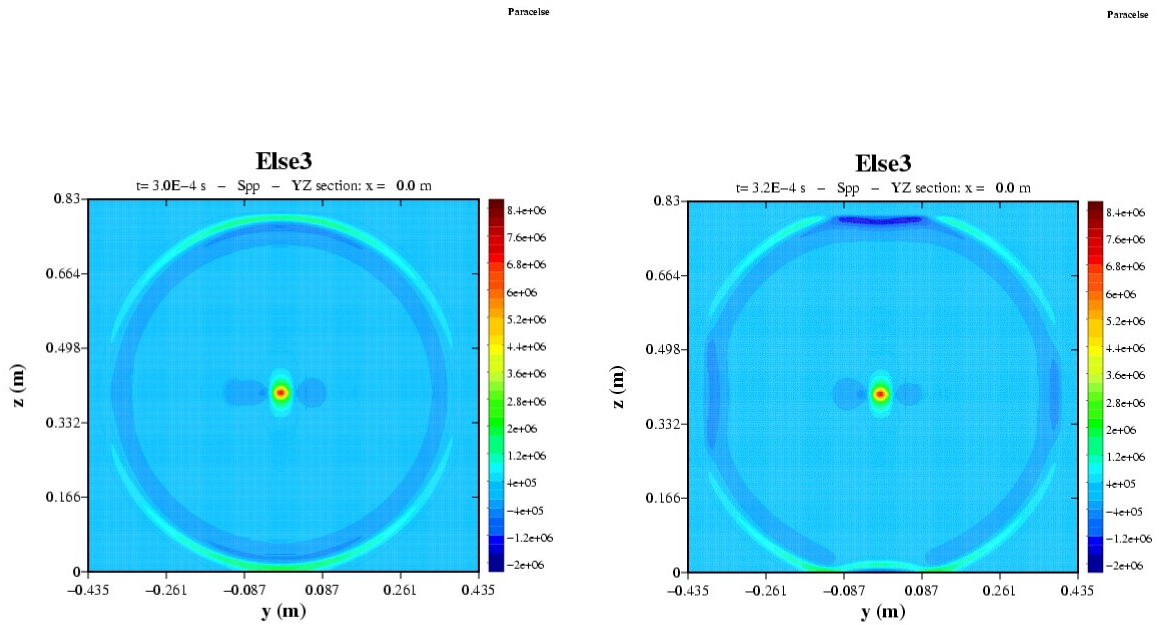


Figure 21 Pressure distribution in a section of the target (Pa)

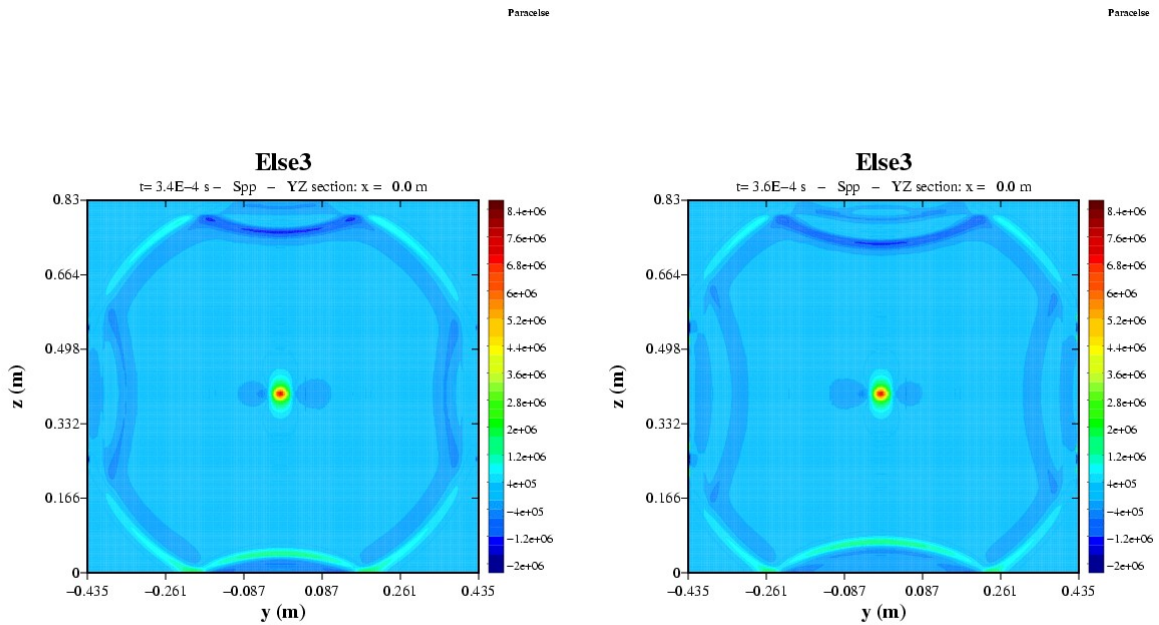


Figure 22 Pressure distribution in a section of the target (Pa)

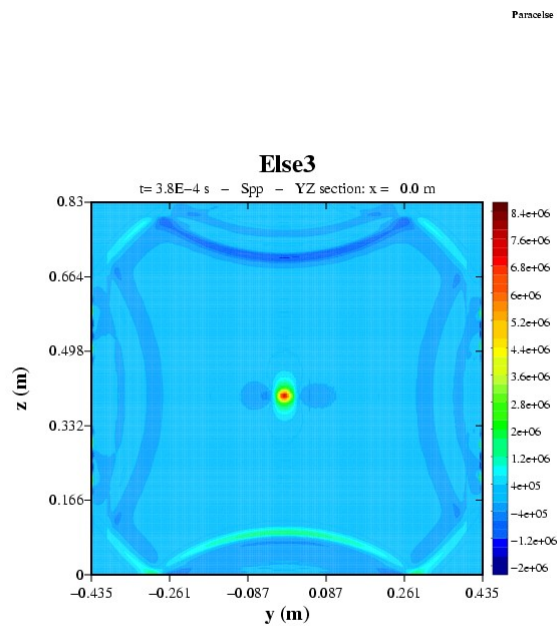


Figure 23 Pressure distribution in a section of the target (Pa)

The wave propagation in the target section is evident in the plots from Figure 24 to Figure 28 where the y and z components of the displacements are shown at the same times of the previous pressure plots.

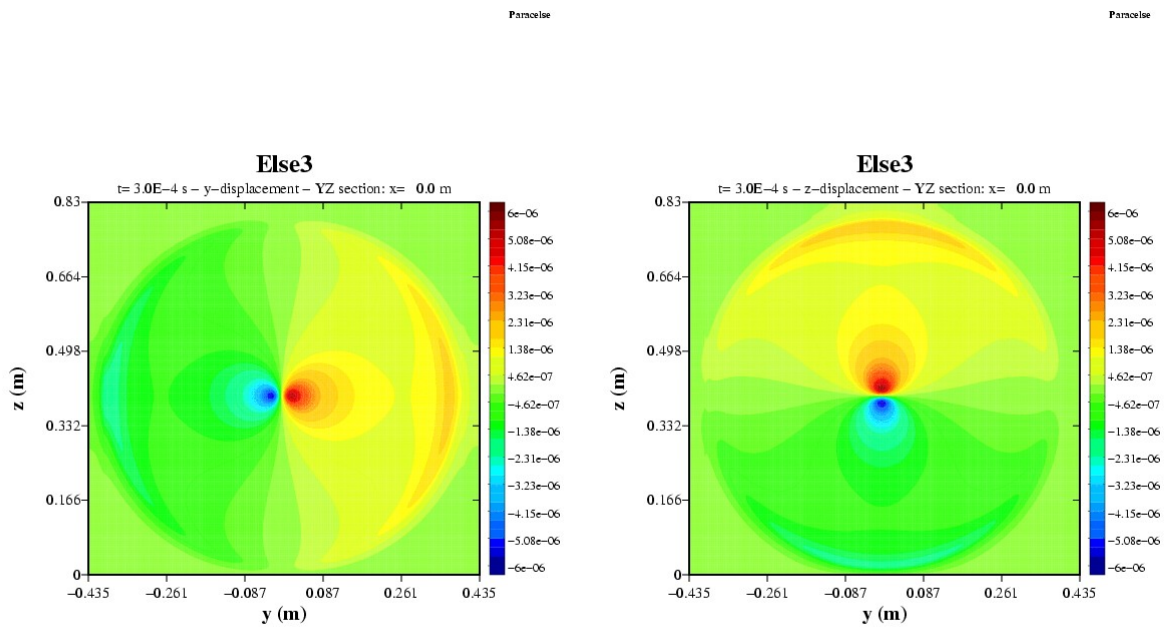


Figure 24 Displacements in the target section in Y and Z directions (m)

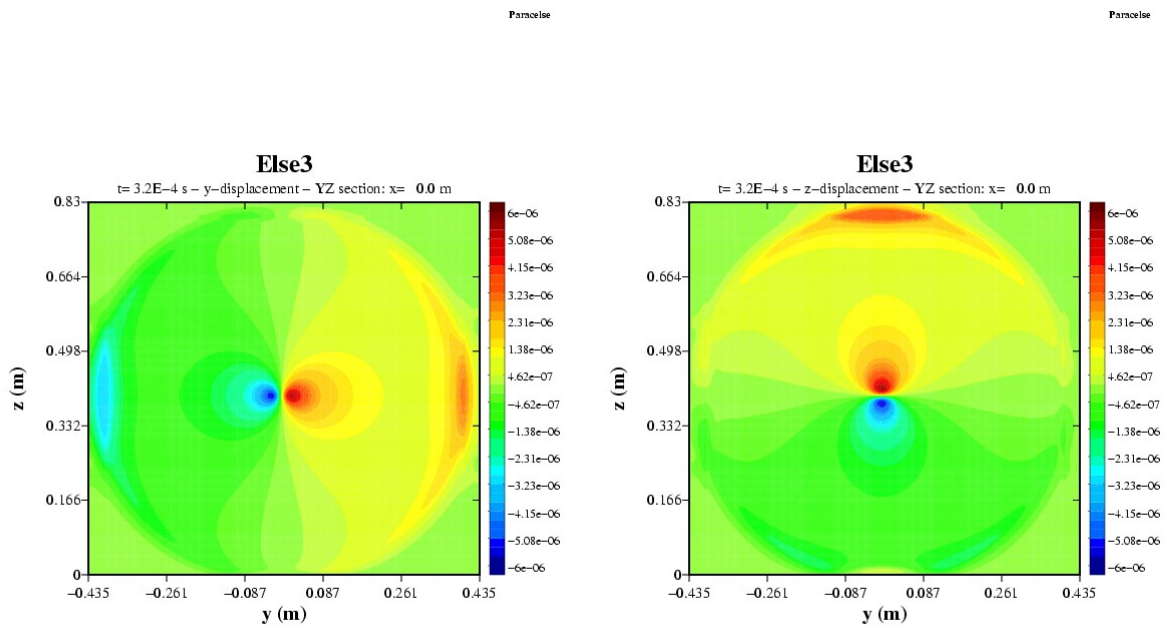


Figure 25 Displacements in the target section in Y and Z directions (m)

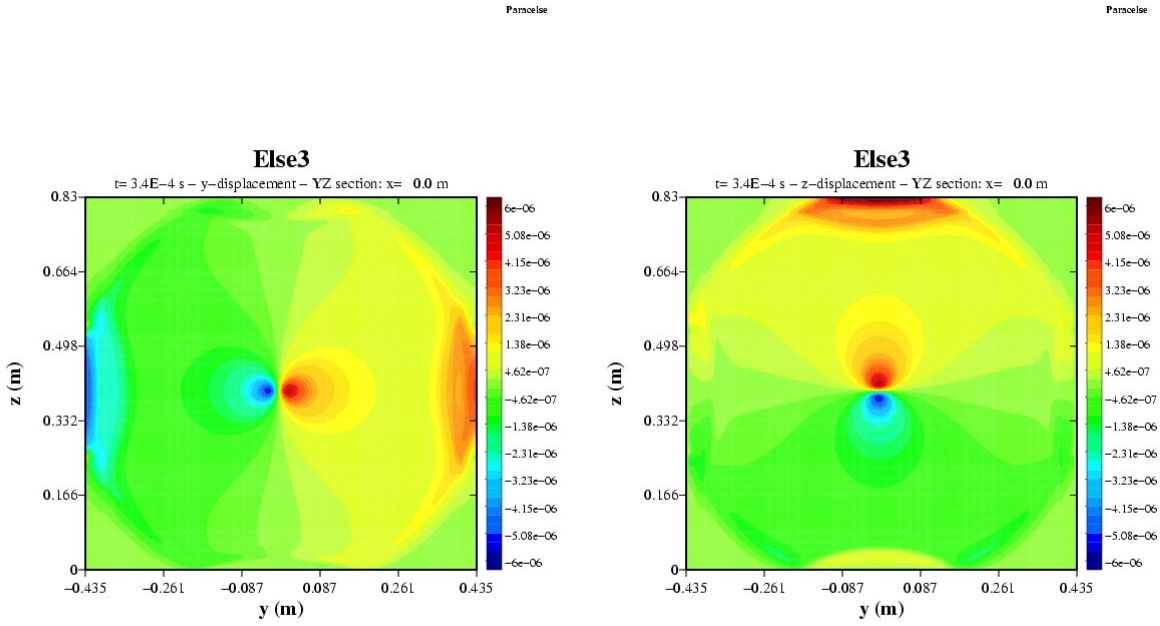


Figure 26 Displacements in the target section in Y and Z directions (m)

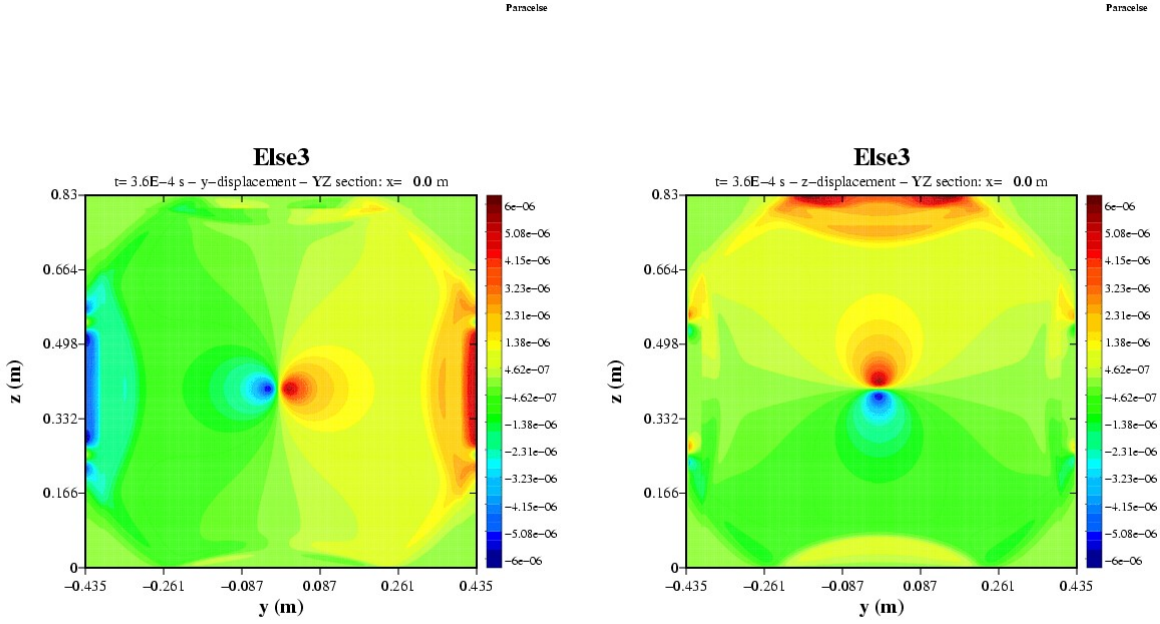


Figure 27 Displacements in the target section in Y and Z directions (m)

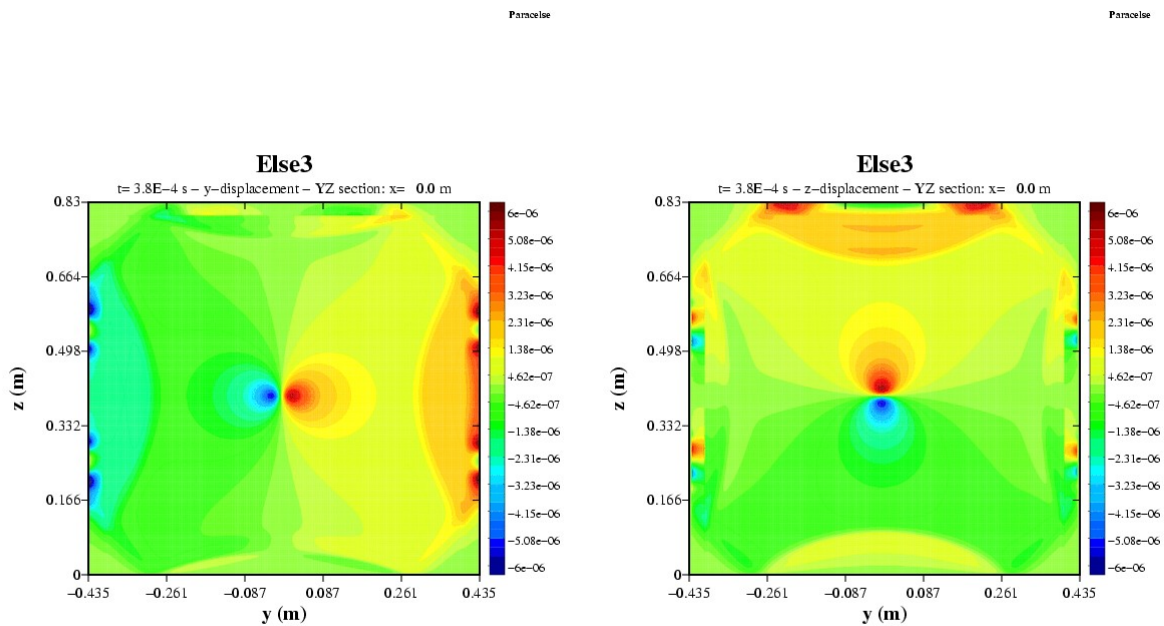


Figure 28 Displacements in the target section in Y and Z directions (m)

## 7 Conclusions

The simulation of the propagation of elastic waves induced by the PS beam into the TOF target has been performed.

The spectral element code ELSE was used, allowing to calculate displacements, pressures and stresses inside the material due to beam energy deposition and consequent wave propagation. Fluka simulation results were used as input for a 3D analysis of the central block and a 2D analysis of a section of the target.

The results showed that the highest pressure values are confined to the points where the energy of the beam is deposited, having a distribution similar to that of the energy density and the temperature increase. Pressure waves departing from the center of the target are not characterized by much high pressure values and rapidly lose intensity as the wave travels away from the center of the block.

The Von Mises equivalent stresses are much lower than the pressure values and are maximum in the energy deposition area. The points near the wave front do not show much high values as long as the wave is confined in the lead block, and do not appear to be critical for the block stability.

The analysis of the section of the block, even with all the approximations that has been necessary to adopt, evidenced how the wave inside the lead can give origin to other “secondary” waves in the water surrounding it and in the aluminum vessel, showing an amplification effect for the displacements.

	Simulation of the elastic wave propagation induced by the PS beam into the TOF target at CERN	TOF MSS Prj FINAL REPORT	Page 27/27
---	---	--------------------------------	------------

It is clear that a more detailed analysis should be necessary to study the wave propagation in the air surrounding the target equipment, anyway surface movements of these amplitude have appeared in some cases to be responsible of an high level noise [4].

## 8 Acknowledgements

The comments and suggestions of researchers of EA Group at CRS4 helped improving this paper significantly, and we would also like to thank Veronique Lacoste, and the people at the CERN for their contribution and scientific support.

This work has been partly supported by Sardinia Region Authorities.

## 9 References

- [1] S. Andriamonje et al., “Neutron TOF Facility (PS 213) - Technical Design Report”, CERN/INTC/2000-004, 6 march 2000.
- [2] E. Faccioli, F. Maggio, R. Paolucci, A. Quarteroni, “2D and 3D elastic wave propagation by a pseudo spectral domain decomposition method” Journal of Seismology, Vol. 1 No. 3 Nov. 1997
- [3] C. Aragonese, S. Buono, L. Maciocco, V. Moreau, L. Sorrentino, “Thermal analysis of the TOF lead target at CERN”, CRS4 Technical report.
- [4] R. Freymann, “Acoustic applications in vehicle engineering”, Fluid-Structure interactions in acoustics, SpringerWienNewYork, 1999